Molecular Crystals and Liquid Crystals Science and Technology. Section A. Molecular Crystals and Liquid Crystals

Publication details, including instructions for authors and subscription information:
http://www.tandfonline.com/loi/gmcl19

Beam Propagation Method Modelling of Zenithal Bistable Nematic Devices: Analysis and Assessment

Emmanouil E. Kriezis [a] & Steve J. Elston [a]

[a] University of Oxford, Department of Engineering Science, Parks Road, Oxford, OX1 3PJ, United Kingdom

Version of record first published: 24 Sep 2006

To cite this article: Emmanouil E. Kriezis & Steve J. Elston (2001): Beam Propagation Method Modelling of Zenithal Bistable Nematic Devices: Analysis and Assessment, Molecular Crystals and Liquid Crystals Science and Technology. Section A. Molecular Crystals and Liquid Crystals, 359:1, 277-288

To link to this article: http://dx.doi.org/10.1080/10587250108035587

Mol. Cryst. and Liq. Cryst., 2001, Vol. 359, pp. 277-288
Reprints available directly from the publisher
Photocopying permitted by license only

Beam Propagation Method Modelling of Zenithal Bistable Nematic Devices: Analysis and Assessment

EMMANOUIL E. KRIEZIS and STEVE J. ELSTON

University of Oxford, Department of Engineering Science Parks Road, Oxford OX1 3PJ, United Kingdom

Modelling of liquid crystal optics is commonly based on variants of matrix-type solvers, which are ideally suited for addressing light wave propagation in stratified anisotropic media. Liquid crystal devices with complex director structures on the micron scale require more rigorous methods for predicting their optical response. Two potential candidate methods exist: the Beam Propagation Method and the Finite-Difference Time-Domain Method. The scope of this paper is to apply the former and assess its accuracy against the latter, which is considered to be more general. The analysis and assessment is focused on Zenithal Bistable Nematic devices.

Keywords: Beam Propagation Method; Liquid Crystals; ZBN

INTRODUCTION

Zenithal Bistable Nematic (ZBN) devices are a promising technology characterised by high mechanical endurance combined with fast switching response. Based on the lithographic recording of a grating structure on the supporting surfaces, and exhibiting a pitch with a typical value of around one micron [1], these devices exhibit an optical response which cannot be satisfactorily modelled by the usual matrix-type

solvers. An alternative approach to the optical modelling is possible through the application of more refined optical wave propagation methods, accounting for structure variation in more than one dimension, such as the Beam Propagation Method (BPM). The BPM is considered to be the ultimate tool in guided wave optics and its applicability has recently been extended to bulk anisotropic media, under the conditions met in liquid crystal structures [2,3].

To suit the geometric requirements of such devices, a wide-angle variant of the BPM is developed to correctly account for light wave components propagating off axis, and is also combined with Periodic Boundary Conditions (PBC). This periodic vector BPM has a lot of attractive features, namely, the ability to cope with media varying in more that one dimension, very fast execution time as it determines the spatial field envelope, correct consideration of the anisotropy, and efficient enforcement of the PBC. Unfortunately, even in its wide-angle variant, the method is not capable of accurately resolving light wave components propagating at ultra-wide angles off axis; conditions that can arise in grating supported ZBN devices.

Here we provide an in-depth assessment of the accuracy provided by the periodic vector BPM, when light propagation within ZBN cells is addressed. The assessment is based on additional simulations carried out by a purely numerical method that directly solves Maxwell's equations in space and time, the Finite-Difference Time-Domain (FDTD) method [4-6]. No approximations, apart from the numerical discretisation, are present in the FDTD method. The normalised transmitted optical intensity between polarising elements, as well as the diffraction efficiencies of the various diffracted orders are compared for both methods. Expected limitations are pointed out, and the margins for safe application of BPM are identified.

CONCISE MATHEMATICAL DESCRIPTION OF PERIODIC BEAM PROPAGATION METHOD

A schematic representation of a ZBN is depicted in figure 1. The director is always oriented within the zenithal plane (xOz), resulting in a purely tilted profile ($\hat{n} = \cos\theta\,\hat{x} + \sin\theta\,\hat{z}$). In a two-dimensional approach $\theta = \theta(x,z)$, and keeping in mind the absence of twist, a natural decomposition of fields into purely ordinary (H_x, E_y, H_z) and

purely extra-ordinary (E_x, H_y, E_z) waves is possible. Therefore, a vector BPM can be formulated for the extra-ordinary wave based on a single scalar quantity, which is the transverse magnetic field component H_y.

As the mathematical formulation will closely follow the one developed in [3], only the salient points will be presented here.

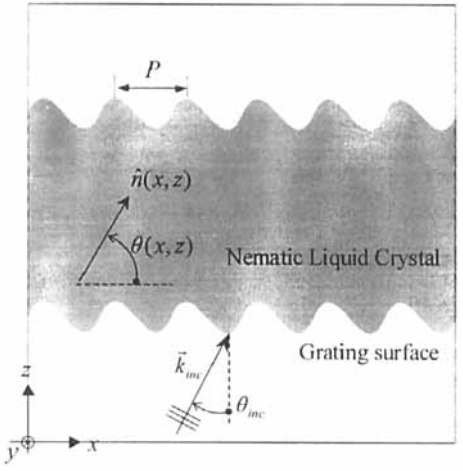

FIGURE 1 Schematic representation of a Zenithal Bistable Nematic cell.

It can be shown that the magnetic field component H_y satisfies the following partial differential equation, which is developed from Maxwell's equations:

$$\varepsilon_{zz}^{\Delta}\frac{\partial^2 H_y}{\partial z^2}+\left(\frac{\partial \varepsilon_{xz}^{\Delta}}{\partial x}+\frac{\partial \varepsilon_{zz}^{\Delta}}{\partial z}\right)\frac{\partial H_y}{\partial z}+\varepsilon_{xx}^{\Delta}\frac{\partial^2 H_y}{\partial x^2}+\left(\frac{\partial \varepsilon_{xx}^{\Delta}}{\partial x}+\frac{\partial \varepsilon_{xz}^{\Delta}}{\partial z}\right)\frac{\partial H_y}{\partial x}+$$
$$2\varepsilon_{xz}^{\Delta}\frac{\partial^2 H_y}{\partial x \partial z}+\omega^2\mu_0 H_y=0 \quad ; \quad \varepsilon_{\alpha\beta}^{\Delta}=\frac{\varepsilon_{\alpha\beta}}{|\tilde{\varepsilon}|} \quad ; \quad \alpha,\beta=x,z \qquad (1)$$

Following the common BPM practise we decompose the field into a spatial envelope multiplied by a fast varying reference exponential term,

i.e., $H_y(x,z) = \mathcal{H}_y(x,z)e^{-jk_{ref}z}$. Substituting this expression into equation (1) leads to the partial differential equation satisfied by the field envelope:

$$\varepsilon_{zz}^{\Delta}\frac{\partial^2 \mathcal{H}_y}{\partial z^2} + R\frac{\partial \mathcal{H}_y}{\partial z} + S\frac{\partial^2 \mathcal{H}_y}{\partial x \partial z} + P\frac{\partial^2 \mathcal{H}_y}{\partial x^2} + Q\frac{\partial \mathcal{H}_y}{\partial x} + T\mathcal{H}_y = 0 \qquad (2)$$

The quantities P,Q,R,S,T appearing in the previous equation are functions of both spatial directions (x,z). As equation (2) is still hard to solve numerically in an efficient way, it will be used as the basis for deriving a wide-angle approximation [7]. The wide-angle approximation is a partial differential equation of parabolic type, which admits an efficient numerical implementation, and also fortunately is not restricted to the paraxial limit (which is simply obtained by omitting the first term of equation (2)). In compact form the wide-angle counterpart of equation (2) is written as:

$$\left(R + S\frac{\partial}{\partial x} - \varepsilon_{zz}^{\Delta}\frac{A}{R}\right)\frac{\partial \mathcal{H}_y}{\partial z} = -A\mathcal{H}_y \qquad (3)$$

$$A(\partial/\partial x, \partial^2/\partial x^2, x, z) \equiv P(x,z)\partial^2/\partial x^2 + Q(x,z)\partial/\partial x + T(x,z) \qquad (4)$$

The final step in the development of the appropriate BPM involves the discretisation of equation (3) using an implicit Crank-Nicolson scheme. The later results is a sparse linear system involving as unknowns the field envelope values at plane $z = (r+1)\delta z$:

$$\left[\mathbf{Y}^{r+1/2}\right]\left[\mathcal{H}_y^{r+1}\right] = \left[\mathbf{W}^{r+1/2}\right]\left[\mathcal{H}_y^{r}\right] \qquad (5)$$

As naturally expected the boundary conditions used for the ZBN are periodic ones. Therefore, the field patterns will replicate themselves from period to period, apart from a phase shift, which is equal to the phase shift of the incident plane wave.

NUMERICAL SIMULATIONS

Numerical simulations are based on the director profiles calculated in [1]. A blazed anti-parallel relief type grating is written on both supporting surfaces, having a profile expressed by:

$$z(x) = \frac{h}{2}\sin\left(\frac{2\pi x}{P} + A\sin\left(\frac{2\pi x}{P}\right)\right) \tag{6}$$

Two stable zero-field patterns are found to exist, corresponding to a low and high tilt state. The low and high tilt states are shown in figure 2.

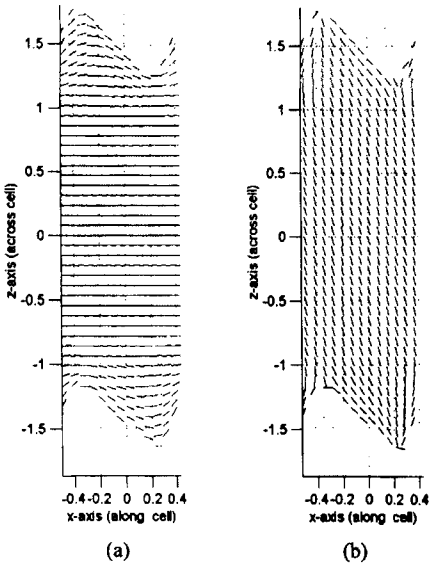

FIGURE 2 Zero-field patterns for a $3.75\mu m$ thick ZBN device with a $1\mu m$ spatial period blazed grating on the upper and lower supporting surfaces (asymmetry factor $A = 0.5$). (a) Low tilt state; (b) High tilt state.

The director profiles shown in figure 2 are analysed by applying the periodic BPM outlined in section 2. Typical nematic liquid parameters are used: $n_0 = 1.5$, $n_e = 1.6$, together with an incident light wavelength of $\lambda = 650nm$. Figure 3 presents the simulation outcome by plotting the real optical power flow $P_R = \frac{1}{2}\mathrm{Re}\{\mathbf{E} \times \mathbf{H}^*\}$ for the propagating extra-ordinary wave. Interest is focused on the extra-ordinary wave, as the ordinary wave is not influenced by the anisotropy, and only senses the ordinary refractive index.

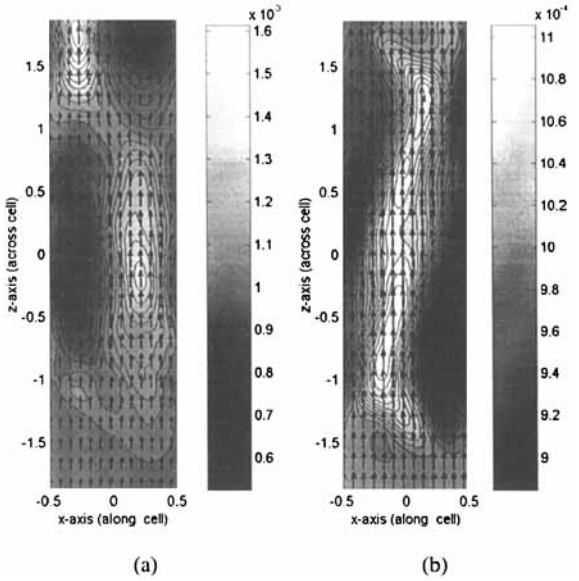

FIGURE 3 Real power flow corresponding to the propagating extra-ordinary wave, when the ZBN is illuminated at normal incidence. (a) Low tilt state; (b) High tilt state.

As can be seen form figure 3, the low and high tilt states lead to two optically distinct field distributions, which can be used advantageously for the bistable device operation. These field distributions, together with the field distribution of the ordinary wave

can be used to determine all electromagnetic field quantities of interest, such as the normalised transmitted optical intensity between polarising elements, or the far field. The critical question is how accurate these results are, as they are obtained by solving equation (3), which is a wide-angle variant of equation (2), and the following section tries to answer this question. It should however be clear that although equation (2) represents a forward only solution, it completely and consistently describes the off-axis propagation of the extra-ordinary wave.

ASSESMENT OF PERIODIC VECTOR BPM AND DISCUSSION

All assessments will be performed by comparing the simulation outcome with that from the Finite-Difference Time-Domain (FDTD) method, which has also recently been introduced to the optical modelling of liquid crystal devices [4-6]. FDTD is a purely numerical method that directly solves Maxwell's equations, both in space and time. In space a staggered grid is used based on the Yee cell, whereas time advancing is performed by a fully explicit leap frog scheme. No assumptions, apart of the numerical discretisation, are present when applying the FDTD method. Therefore, the FDTD outcome will serve as a reference solution.

A first step towards the BPM accuracy assessment is a comparison in the transmitted near field optical intensity, when the ZBN device is viewed between crossed ideal polarising elements. Polarising elements are placed at $\phi_{in} = 45^o$ for the entrance polariser (lower surface) and $\phi_{out} = -45^o$ for the exit analyser (upper surface). Figure 4 plots the normalised transmitted intensity for the low tlit state (shown in figure 2a) as calculated by the BPM and the FDTD method for various angles of incidence $\theta_{inc} = 0^o, 15^o, 30^o, 45^o$, all measured within the surrounding isotropic material composing the grating surface. The grating material is assumed to have a refractive index equal to the ordinary refactive index. As can be seen the maximum difference (error) in the transmitted optical intensity is minimal up to 15^o, it is approximately equal to 3.3% for 30^o, and reacheas a value of 6.1% for 45^o.

A further in depth view of the errors involved is available by plotting the diffraction efficiencies of the lower order propagating

modes $(0,\pm1)$ for the extra-ordinary wave versus the angle of incidence. In the case of the BPM only the transmitted diffraction efficiencies can be computed as the BPM represents a forward only solution. In the case of the FDTD both transmitted and reflected diffraction efficiencies are obtained, and therefore, one can have in principle an estimate of the error introduced in the BPM simulation by totally ignoring the counter-propagating field. Figure 5 plots the diffraction efficiencies $(e_m, m = 0,\pm1)$ versus the angle of incidence, where the later spans the interval up to $[-45^o, 45^o]$. The diffraction efficiency e_m is defined as the ratio of the power carried by the m-th diffracted order divided by the incident power.

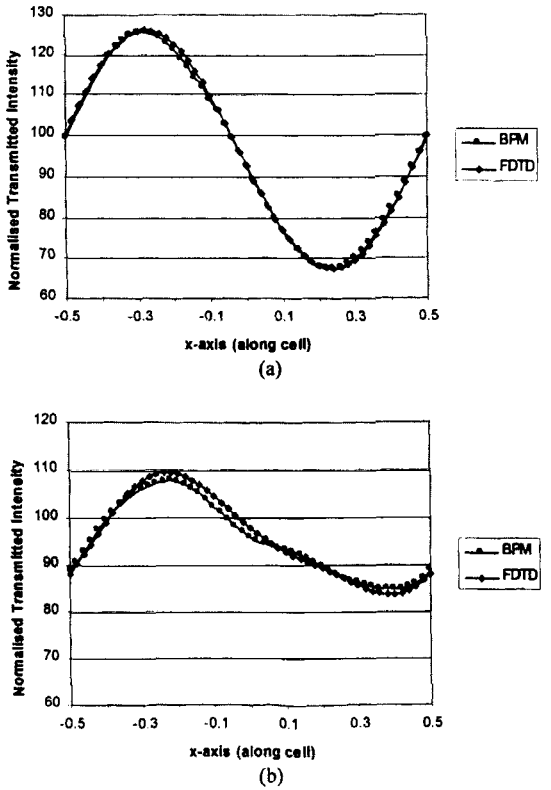

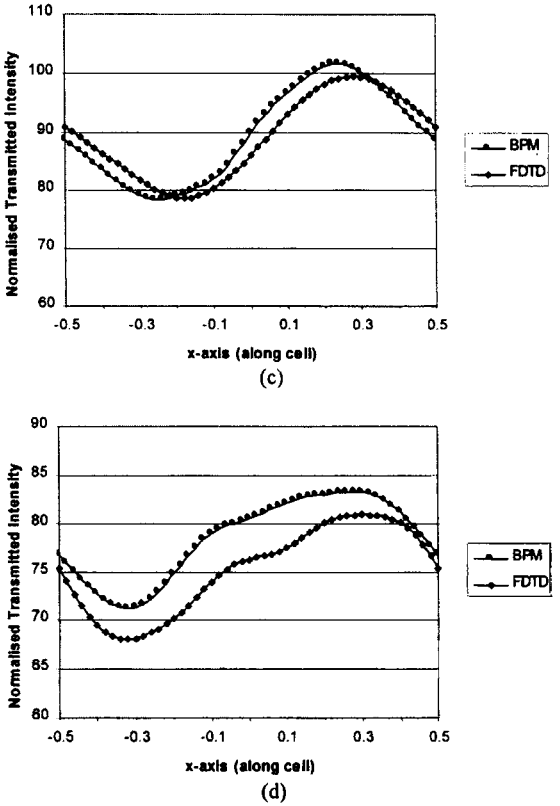

FIGURE 4 Normalised transmitted near field optical intensity between crossed polarisers for the low tilt state of figure 2a. The supporting grating material is considered to be isotropic with $n_s = n_o$. (a) $\theta_{inc} = 0^o$; (b) $\theta_{inc} = 15^o$; (c) $\theta_{inc} = 30^o$; (d) $\theta_{inc} = 45^o$.

A satisfactory agreement exists between both methods for the zeroth diffracted order (direct wave), as shown in figure 5a, leading to small relative errors. In the case of the higher diffracted orders $m = \pm 1$ the relative errors can be more pronounced under certain circumstances, although, the general trend of the BPM simulation follows that of the

FDTD method. For instance in figure 5b for $\theta_{inc} = -25^{o}$ the error is excessive as the diffracted order $m = -1$ propagates at $\theta_{-1} = -58.8^{o}$, clearly violating the wide-angle approximation, and therefore, the diffraction efficiency is not accurately predicted by applying the BPM. The reflected field has been estimated by the FDTD method and was found to be very weak. As a consequence, neglecting the reflected field in the BPM was not a source of significant error, compared to the error introduced by the violation of the wide-angle approximation.

Another point that should receive some attention is that of numerical dissipation. Both methods are found to exhibit numerical dissipation equivalent to few percent units. In the FDTD method reducing the spatial steps results in monotonic numerical dissipation reduction. In the BPM the numerical dissipation is a more complex function of the axial step and the controlling parameter of the implicit Crank-Nicolson scheme used. It is not uncommon to find for the BPM that stability is gained at the expense of increased numerical dissipation.

All comparisons were based on the low tilt state; for the high tilt state similar observations hold.

The salient features of both methods are summarised in table 1.

	WIDE-ANGLE BPM	FDTD METHOD
Discretisation	Field envelope in space	Instantaneous field values in space and time
Type of Grid	Conventional (not-staggered) FD grid	Staggered grid consisting of Yee cells
Numerical Scheme	Implicit Crank-Nicolson scheme	Fully explicit
Stability	Conditionally stable depending on scheme parameter	Conditionally stable depending on Courant stability criterion
Reflections	Not included	Fully included
Boundary Conditions	Periodic boundary conditions	Periodic boundary conditions with Perfectly Matched Layer on upper and lower ends
Propagation off-axis	Limited to few tens of degrees (max up to 45°)	Ultra-wide angles up to grazing
Computational burden	Extremely moderate as it works with the spatial field envelope	Significantly increased requiring Yee cells with dimensions of at least λ/20

TABLE 1 Features of WA-BPM and FDTD method.

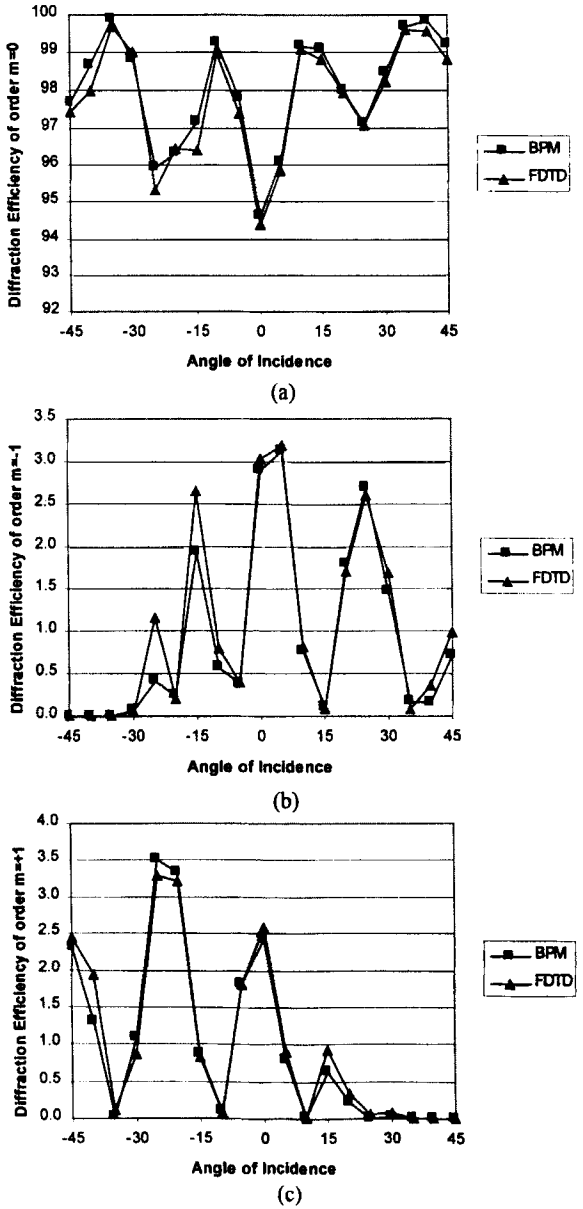

FIGURE 5 Diffraction efficiencies versus angle of incidence. (a) $m = 0$; (b) $m = -1$; (c) $m = +1$.

CONCLUSIONS

A periodic wide-angle vector BPM has been presented and applied to a typical ZBN device. The numerical results were assessed by comparison with the numerical results of the FDTD method. The later is considered to represent a more general and accurate but also more computationally intensive solution. Comparisons were carried out for the near-field transmitted intensity and the lower order diffraction efficiencies. The margins for the safe application of this specific wide-angle BPM require that the incident field (and as a consequence the lowest diffracted order) as well as any of the higher diffracted orders carrying a significant fraction of the transmitted optical power should not violate the wide-angle approximation. This wide-angle limit is equivalent to few tens of degrees off-axis propagation (in essence less that 45°). It is obvious that the reflected field should also be negligible, which seems to be the case for this type of device. If the above conditions are met the results from the BPM agree favourably with the FDTD method prediction, which is a strong indication of reliability.

Acknowledgements
The authors wish to acknowledge the financial support of the EPSRC. Furthermore, they wish also to acknowledge Dr. C. V. Brown for providing the director profiles used throughout the numerical simulations.

References

[1] C. V. Brown, G. P. Bryan-Brown, and V. C. Hui, *Mol. Cryst. Liq. Cryst.*, **301,** pp. 163–168, (1997).
[2] E. E. Kriezis and S. J. Elston, *J. Modern Optics*, **46,** pp. 1201–1212, (1999).
[3] E. E. Kriezis and S. J. Elston, *Liquid Cryst.*, **26,** pp. 1663–1669 (1999).
[4] B. Witzigmann, P. Regli, and W. Fichtner, *J. Opt. Soc. Am. A.*, **15,** pp. 753–757 (1998).
[5] E. E. Kriezis and S. J. Elston, *Optics Comm.*, **165,** 1–3, pp. 99–105, (1999).
[6] C. M. Titus, P. J. Bos, and J. R. Kelly, *SID 99 Digest*, pp. 624–627 (1999)..
[7] G. R. Hadley, *Optics Letters*, **17,** pp. 1426–1428, (1992).